

Proteolysis of the Exodomain of Recombinant Protease-Activated Receptors: Prediction of Receptor Activation or Inactivation by MALDI Mass Spectrometry[†]

Damarys Loew,[‡] Christelle Perrault,[§] Martine Morales,[§] Sylvie Moog,[§] Catherine Ravanat,[§] Simone Schuhler,[§] Rosaria Arcone,^{||} Concetta Pietropalo,^{||} Jean-Pierre Cazenave,[§] Alain van Dorsselaer,[‡] and François Lanza^{*,§}

Laboratoire de Spectrométrie de Masse Bio Organique, Université Louis Pasteur, Strasbourg, France, INSERM U311, Etablissement Français du Sang-Alsace, Strasbourg, France, and Dipartimento di Biochimica e Biotecnologie Mediche, Università "Federico II", Naples, Italy

Received February 11, 2000; Revised Manuscript Received June 6, 2000

ABSTRACT: Protease-activated receptors (PARs) mediate cell activation after proteolytic cleavage of their extracellular amino terminus. Thrombin selectively cleaves PAR1, PAR3, and PAR4 to induce activation of platelets and vascular cells, while PAR2 is preferentially cleaved by trypsin. In pathological situations, other proteolytic enzymes may be generated in the circulation and could modify the responses of PARs by cleaving their extracellular domains. To assess the ability of such proteases to activate or inactivate PARs, we designed a strategy for locating cleavage sites on the exofacial NH₂-terminal fragments of the receptors. The first extracellular segments of PAR1 (PAR1E) and PAR2 (PAR2E) expressed as recombinant proteins in *Escherichia coli* were incubated with a series of proteases likely to be encountered in the circulation during thrombosis or inflammation. Kinetic and dose–response studies were performed, and the cleavage products were analyzed by MALDI-TOF mass spectrometry. Thrombin cleaved PAR1E at the Arg41–Ser42 activation site at concentrations known to induce cellular activation, supporting a native conformation of the recombinant polypeptide. Plasmin, calpain and leukocyte elastase, cathepsin G, and proteinase 3 cleaved at multiple sites and would be expected to disable PAR1 by cleaving COOH-terminal to the activation site. Cleavage specificities were further confirmed using activation site defective PAR1E S42P mutant polypeptides. Surface plasmon resonance studies on immobilized PAR1E or PAR1E S42P were consistent with cleavage results obtained in solution and allowed us to determine affinities of PAR1E–thrombin binding. FACS analyses of intact platelets confirmed the cleavage of PAR1 downstream of the Arg41–Ser42 site. Mass spectrometry studies of PAR2E predicted activation of PAR2 by trypsin through cleavage at the Arg36–Ser37 site, no effect of thrombin, and inactivation of the receptor by plasmin, calpain and leukocyte elastase, cathepsin G, and proteinase 3. The inhibitory effect of elastase was confirmed on native PAR1 and PAR2 on the basis of Ca²⁺ signaling studies in endothelial cells. It was concluded that none of the main proteases generated during fibrinolysis or inflammation appears to be able to signal through PAR1 or PAR2. This strategy provides results which can be extended to the native receptor to predict its activation or inactivation, and it could likewise be used to study other PARs or protease-dependent processes.

Proteases play a central role in mediating cellular migration and invasion by cleaving matrix proteins and also through direct cellular effects (1). Protease-activated receptors (PARs)¹ are members of an emerging family of receptors which are activated by proteases generated during hemostasis and inflammatory processes. The best examples of PARs are the

cellular receptors for thrombin (2), a serine protease generated by the coagulation cascade (3). Thrombin activates various types of cells in the vasculature like platelets and endothelial cells. Three such receptors have been identified. PAR1 was the first PAR to be cloned and is present in human platelets and endothelial cells (4). PAR3 has been cloned from rodent cells (5, 6) and is active in rodent platelets but only weakly expressed in the human vasculature. Finally, the recently cloned PAR4 has been described in different tissues and cells, including platelets (7, 8). A fourth member of the family, PAR2, does not respond to thrombin and is absent from platelets, but has been described in endothelial cells especially in inflammatory situations (9–12). The proposed mode of action of PARs involves cleavage at a specific site in the NH₂-terminal exodomain to expose a new NH₂ terminus, which in turn interacts intramolecularly with exofacial loops of the receptor and promotes intracellular signaling (2).

[†] The Conseil Régional d'Alsace is acknowledged for a financial support in the acquisition of a Biflex II Bruker MALDI-TOF mass spectrometer.

* To whom correspondence should be addressed: INSERM U.311, Etablissement Français du Sang-Alsace, 10 rue Spielmann, BP 36, 67065 Strasbourg Cédex, France. Telephone: +33-388-21-25-25. Fax: +33-388-21-25-21. E-mail: francois.lanza@etss.u-strasbg.fr.

[‡] Université Louis Pasteur.

[§] Etablissement Français du Sang-Alsace.

^{||} Università "Federico II".

¹ Abbreviations: FACS, fluorescence-activated cell sorting; GST, glutathione S-transferase; LC, liquid chromatography; MALDI-TOF, matrix-assisted laser desorption/ionization time-of-flight; MoAb, monoclonal antibody; PAR, protease-activated receptor.

In addition to thrombin, other proteases are generated following vessel wall injury. The plasma protease plasmin promotes dissolution of the fibrin clot (13); activated neutrophils release serine proteases such as elastase or cathepsin G from their azurophilic granules (14, 15), while stimulated platelets express at their surface different metalloproteinases such as calpain (16, 17). These proteases have the ability to activate PARs if cleavage occurs at the activating site or on the contrary to inactivate them if cleavage occurs at a COOH-terminal site. Precise determination of the site of cleavage of these proteases would thus allow simple prediction of their activating or inhibitory potential in cellular systems.

In the study presented here, we sought to determine the effects of a number of proteases on PAR1 and PAR2. These two receptors were the first members of the family to be identified and were selected because of their common presence in the vasculature and distinct protease specificities. A classical approach to studying cleavage involves the use of synthetic peptide substrates designed from the coding sequence, which are HPLC-separated after cleavage and analyzed by amino acid sequencing or mass spectrometry. This procedure has been employed to identify the cleavage sites of thrombin and neutrophil proteases on the NH₂-terminal exodomain of PAR1 (18–20). The approach nevertheless has limitations due to its use of short peptides, since the specificity of proteases depends not only on the primary amino acid sequence of the substrate but also on its native conformation, which is better preserved in larger polypeptides.

Therefore, we chose to use larger recombinant proteins to obtain a cleavage profile that is more accurate than that with short peptides. The entire NH₂-terminal exodomains of PAR1 and PAR2 were produced in *Escherichia coli* and tested for cleavage by selected proteases. Previous studies of PAR1 have shown that this NH₂-terminal segment contains all the information required for efficient recognition and cleavage by thrombin, its physiologic agonist (21, 22). In addition to thrombin and trypsin, the preferred agonists of PAR1 and PAR2, respectively, we tested the effects of plasmin, calpain, and the leukocyte proteases elastase, cathepsin G, and proteinase 3, all of which are enzymes generated in thrombotic or inflammatory situations. The exact sites of cleavage and their sensitivity were determined by analyzing the cleaved samples using the rapid and sensitive technique of matrix-assisted laser desorption/ionization (MALDI) mass spectrometry. In addition, cleavage specificities and the affinity of PAR1 for thrombin were studied on the immobilized PAR1 exodomain using surface plasmon resonance.

EXPERIMENTAL PROCEDURES

Materials. Reagents and chemicals used for DNA analyses were molecular biology grade and free of DNase and RNase activities. Restriction enzymes were purchased from New England Biolabs (Ozyme, Montigny Le Bretonneux, France), and oligonucleotide primers were synthesized in an Oligo 1000 synthesizer (Beckman, Gagny, France). Purified human α -thrombin was obtained from the Etablissement Français du Sang-Alsace (Strasbourg, France), while recombinant hirudin was a generous gift from A. Pavirani (Transgène SA,

Strasbourg, France). PGI₂ was from Sigma Chemicals (St. Louis, MO), heparin from Hoffmann La Roche (Basel, Switzerland), and Pefablock from Interchim (Montluçon, France). WEDE MoAb against PAR1 and fluorescein isothiocyanate (FITC)-conjugated goat anti-mouse (GAM) F(ab)₂' antibodies were purchased from Immunotech (Luminy, France). Ila-RA MoAb against PAR1 was obtained from Biodesign International (Kennebunk, ME). Trypsin and APMSF were from Boehringer-Roche (Meylan, France); human cathepsin G (CG), elastase (EL), and proteinase 3 were from Athens Research and Technology (Athens, GA), and plasmin and calpain I and II were from Calbiochem (La Jolla, CA). Eglin C was from Bachem (Voisin le Bretonneux, France).

Production of Recombinant PAR1 and PAR2 NH₂-Terminal Exodomains in *E. coli*. cDNA encoding the NH₂-terminal domain of PAR1 (PAR1E, positions 25–99; 4) was amplified by PCR from the pBluescript plasmid containing the entire coding sequence (23). The (+)-strand primer was 5'-ATGGATCCCGGGCCGAGGCCAGAATCAAAGC-3' (P1E5) and the (–)-strand primer 5'-GAAGATGCCTCCGATATTTGACCAGCTCGAGCGC-3' (P1E3), and *Bam*HI and *Xho*I restriction sites were added to P1E5 and P1E3, respectively, for cloning purposes. A Ser to Pro mutation was introduced at position 42 by overlap PCR mutagenesis using oligonucleotides TRESP1 [(+)-5'-CTTAGATCCCAGGCCTTTTCTTCTCAG-3'] and TRESP2 [(–)-5'-CTGAGAA-GAAAAGGCCTGGGATCTAAG-3']. Two separate PCR amplifications were performed on the PAR1 pBluescript vector using the primer pairs P1E5-TRESP2 and P1E3-TRESP1, and the resultant 70- and 180-nucleotide fragments were purified on GeneClean (Bio101, Ozyme). A second PCR was performed by adding 50 ng of each fragment and the primer pair P1E5 and P1E3. The wild-type and mutated fragments were cleaved and inserted in-frame with GST in the *Bam*HI–*Xho*I sites of the pGEX6P3 bacterial expression vector (Amersham-Pharmacia Biotech, Uppsala, Sweden). For surface plasmon resonance studies, a six-His tag was attached at the C-terminus of the constructs. PAR1E and PAR1E S42P fragments amplified with *Bam*HI and *Sal*I sites at their 5' and 3' extremities were inserted in-frame in the *Bam*HI–*Sal*I site of pGEX6P1 containing a six-His coding sequence in the *Sal*I–*Xho*I site. DNA encoding the PAR2 NH₂-terminal domain (PAR2E, positions 31–79; 24) was amplified from human genomic DNA by PCR with the (+)-primer P2E5 (5'-CGGGATCCAGATCTTCTAAAGGAAGAGCCTTATTGG-3') and the (–)-primer P2E3 (5'-GAAAGTACGACGAGTCTTCTTCCAACTCGAGCGG-3'). A Ser to Pro mutation was introduced at residue 37 using the mutating primer MUT1 (5'-CGGGATCCAGATCTTCTAAAGGAAGACCCCTTATTGG-3') for the (+)-strand and the P2E3 primer for the (–)-strand. The wild-type and mutated PAR2E fragments were cleaved and inserted in-frame with GST in the *Bam*HI–*Xho*I sites of pGEX6P3.

All the constructs were checked by DNA sequencing. The vector constructs added five to seven residues NH₂- and COOH-terminal to PAR1E and PAR2E, and these are indicated in the legend of Figure 1. The different recombinant plasmids were transfected first into XL2Blue *E. coli* (Stratagene, Ozyme) to establish the cell lines and then into BL21 cells (Novagen, Madison, WI) for protein expression. Bacterial cell cultures (150 mL) were induced with 0.2 mM IPTG

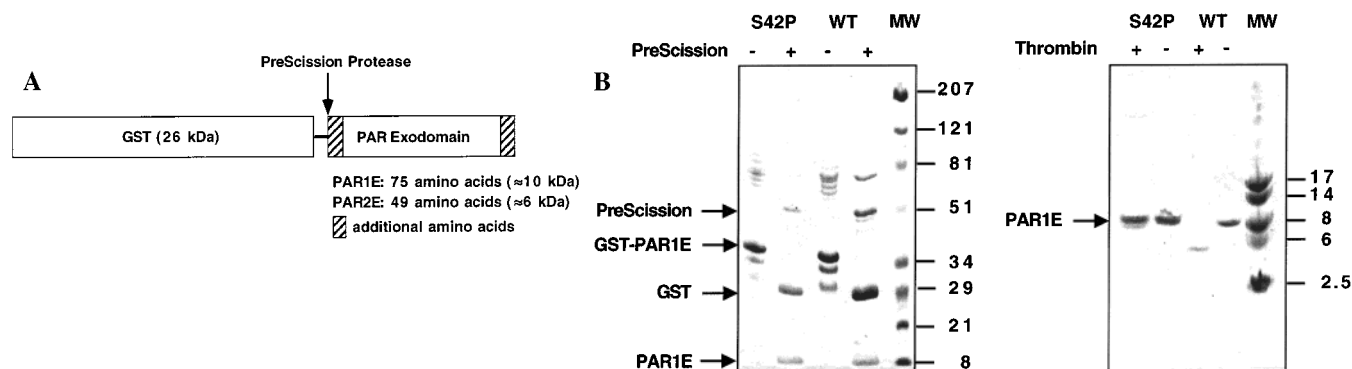


FIGURE 1: Production of recombinant PAR1 and PAR2 NH₂-terminal exodomains in *E. coli*. (A) Schematic representation of the fusion protein between glutathione *S*-transferase (GST, 26 kDa) and the PAR1 or PAR2 exodomain (PAR1E or PAR2E) produced using the PGEX-6P expression vector. PAR1E and PAR2E were released from GST by PreScission cleavage and purified by HPLC as described in Experimental Procedures. The sequences (hatched bars) added at positions NH₂- and COOH-terminal to the constructs due to insertion in the vector are GPLGS and SGRIVTD for PAR1E and GPLGS and TRAAAS for PAR2E, respectively. (B) SDS-PAGE analyses of recombinant GST-PAR1E and PreScission-purified PAR1E. Supernatants from *E. coli* lysates containing wild-type (WT) or Ser42 → Pro (S42P) mutant GST-PAR1E constructs were applied to a glutathione-Sepharose column and eluted with SDS. The two fusion proteins migrated at 36 kDa. Treatment with PreScission liberated wild-type or mutant PAR1E from GST which remained attached to the column (left). WT and S42P both eluted as a single 10 kDa band. Treatment of wild-type PAR1E with thrombin decreased its size to 7 kDa by cleavage at position Arg41 but had no effect on the mutant protein (right).

at 30 °C for 3 h. The cell suspensions were then pelleted and washed once in PBS buffer containing 1× protease inhibitor cocktail (Boehringer), and the final pellets were frozen at −80 °C until purification was carried out. Frozen pellets were transferred to liquid nitrogen for 5 min and disrupted in a Freezer/Mill 6750 SPEXCertiprep (Polylabo, Illkirch, France) using six cycles of 30 s with 15 strokes/s. This disruption technique gave significantly higher yields and less protein degradation than sonication. The resulting powders were resuspended and incubated for 1 h in 30 mL of ice-cold PBS in the presence of protease inhibitors and 1% Triton X-100. After centrifugation at 11 000 rpm for 10 min, the supernatants were added to 5 mL of glutathione-Sepharose 4B beads (Pharmacia) and incubated overnight at 4 °C without agitation. The beads were washed twice in PBS containing protease inhibitors, and the GST fusion proteins were released by adding glutathione and the PARE fragments by incubating with PreScission Protease. Briefly, the PAR exodomains were cleaved from the GST tag while bound to glutathione-Sepharose 4B by digestion of the GST-PAR fusion proteins with PreScission Protease (Amersham-Pharmacia Biotech) according to the manufacturer's instructions.

LC-MS Analyses. The proteins were further purified and analyzed by on-line liquid chromatography and mass spectrometry (LC-MS). The chromatographic equipment comprised an HPLC Alliance system (Waters 2690, separations module) with a diode array detector (Waters 996, photodiode array detector) on a Narrowbore Macherey Nagel Nucleosil 300-5C18 column (2 mm × 125 mm) maintained at 35 °C. The solvent system consisted of 0.1% trifluoroacetic acid and water (solvent A) and 0.08% trifluoroacetic acid and acetonitrile (solvent B), and separation was achieved at 0.25 mL/min using a 1%/min gradient increase in solvent B over the course of 60 min. The column effluent was flow-split at a stainless steel Valco tee (Supelco) which directed approximately 1/15 into a Quattro II mass spectrometer (Micromass Ltd., Altrincham, U.K.), and mass analyses were performed essentially as described previously (25). After purification, the proteins were NH₂-terminally sequenced by

automated Edman degradation on a pulse liquid automatic peptide sequencer (Applied Biosystems model 473A).

Hydrolysis of PAR1 and PAR2 NH₂-Terminal Exodomains. Proteases were reconstituted in saline buffer at a concentration 10 times greater than the working concentration. A 0.5 μL aliquot of the 10× protease solution was incubated at 37 °C with 4.5 μL of HPLC-purified recombinant PAR1E or PAR2E in 100 mM Tris-HCl (pH 8) at a final PAR concentration of 10 μM. Optimal protease concentrations and incubation times were determined in preliminary experiments and are listed in the Results and in Table 1. At various incubation times, a 0.5 μL aliquot of the digestion mixture was quenched in 2% trifluoroacetic acid on the first layer of the mass spectrometer matrix. The matrix and sample were allowed to dry, and the probe was rinsed with 1 μL of 0.1% trifluoroacetic acid (26–29).

Analysis of Protease Cleavage by MALDI-TOF Mass Spectrometry. Cleavage products were analyzed on a Bruker Biflex matrix-assisted laser desorption/ionization time-of-flight mass spectrometer (Bremen, Germany) with improved resolution through delayed ion extraction. Samples were prepared via a two layer method (26, 30), and all studies were performed in the linear or reflector positive mode at an acceleration potential of 20 or 19 kV, respectively. The resolution in the linear mode was approximately 1:2000 with a mass accuracy of 0.1%, and the masses that were determined were therefore average masses. In the reflector mode, where the resolution typically ranged from 1:6000 to 1:6500 with a mass accuracy of better than 0.05%, monoisotopic masses were determined below 6000 Da and average masses above 6000 Da. A majority of peptides resulting from the enzymatic digestions appeared as singly charged, monoprotonated molecular ions at m/z $[M + H]^+$, with occasional doubly and triply protonated ions at m/z $[M + 2H]^{2+}$ and $[M + 3H]^{3+}$.

Surface Plasmon Resonance Analysis. His-tagged PAR1E and PAR1E S42P were immobilized on a nitriloacetic acid sensor chip (NTA) mounted in a Biacore 2000 instrument as described by the manufacturer (Biacore, Uppsala, Sweden) (31). Briefly, 500 μM NiCl₂ in eluent buffer [10 mM HEPES,

Table 1: Protease Cleavage Sites on Recombinant PAR1 and PAR2 NH₂-Terminal Exodomains (PAR1E and PAR2E)^a

	PAR1E		PAR2E	
	early cleavage	late cleavage	early cleavage	late cleavage
thrombin	[41–42]	25–26, 43–44	[36–37]	
trypsin	[41–42], 70–71, 82–83	47–48	34–35, [36–37], 51–52, 72–73	
plasmin	[32–33], 70–71, 76–77	[41–42]	34–35, [36–37]	
cathepsin G	[41–42], 55–56, 69–70	43–44	59–60, 64–65	
elastase	36–37, 72–73, 86–87		76–77	
proteinase 3	36–37, 48–49, 72–73, 92–93	54–55	48–49, 74–75, 75–76, 76–77	
calpain I	32–33, 76–77		55–56, 57–58, 61–62, 62–63, 72–73	
calpain II			59–60	
			45–46, 58–59, 71–72	

^a PAR1E and PAR2E (10 μ M) were incubated in the presence of the different proteases for 30 s to 3 h, and the cleavage products were analyzed directly by MALDI-MS. Early (0–5 min) and late (5 min to 3 h) cleavage sites are listed, and the amino acid positions correspond to the mature proteins according to ref 4 (PAR1) and ref 24 (PAR2). The enzymes were used at the following concentrations: 0.5 unit/mL thrombin, 2.5 nM trypsin, 20 nM plasmin, 20 nM cathepsin G, 20 nM elastase, 20 nM proteinase 3, and 2 units/mL calpain I and II. Cleavage sites given in brackets are absent from the PAR1E S42P and PAR2E S37P mutants (see also Figures 4 and 7).

0.15 M NaCl, 50 μ M EDTA, and 0.005% Surfactant P20 (pH 7.4)] was injected over the course of 1 min at a flow rate of 20 μ L/min followed by injection of His-PAR1E or His-PAR1E S42P (200 nM) in eluent buffer for 15 min at a flow rate of 5 μ L/min. Proteases to be tested were diluted in eluent buffer and injected for 10 min at 25 °C at a flow rate of 5 μ L/min with or without addition of specific inhibitors. The surface was regenerated by injection of 30 μ L of regeneration solution [10 mM HEPES, 0.15 M NaCl, 0.35 M EDTA, and 0.005% Surfactant P20 (pH 8.3)] at a flow rate of 10 μ L/min. The amount of PAR1E bound to the chip and the extent of cleavage were measured by the variation in surface plasmon resonance angle as a function of time and were expressed in resonance units (RU). Binding rate constants for PAR1E–thrombin interaction were determined by immobilizing His-PAR1E and injecting S205A mutant thrombin (32) or by immobilizing His-PAR1E S42P and injecting normal or S205A mutant thrombin at concentrations of 45, 90, and 180 nM and at a flow rate of 50 μ L/min. Kinetic parameters were derived using Biaevaluation 3.0 software. Association rate constants (k_{on}) and dissociation rate constants (k_{off}) were determined from association and dissociation curves, respectively, assuming a one-to-one interaction. The affinity constant K_D was calculated as k_{off}/k_{on} .

Flow Cytometric Studies of Human Platelets. Platelet rich plasma was prepared from acid-citrate-dextrose anticoagulated blood obtained from aspirin-free healthy volunteers, and platelets were washed by sequential centrifugation as previously described (33). The cells were finally resuspended in Tyrode's buffer (pH 7.35) containing 5 mM Hepes, 0.35% human serum albumin, and 2 μ g/mL apyrase and adjusted to a density of 3×10^5 platelets/ μ L. Washed platelets were left untreated or incubated with different proteases as follows: 5 min at 37 °C with 5 units/mL thrombin followed by blockade with 10 units/mL hirudin, 30 min at 37 °C with 100 nM cathepsin G, 100 nM elastase, or 500 nM proteinase 3 followed by blockade with 10 μ g/mL eglin C, or 30 min at 37 °C with 400 nM plasmin or 10 units/mL calpain followed by blockade with 7 \times protease inhibitor cocktail (Boehringer). Prior to flow cytometric analyses, 50 μ L of platelet suspension was incubated with a saturating concentration of purified MoAb at 22 °C for 30 min and then with 0.5 μ g of FITC-GAM at 22 °C for 30 min in the dark. After each incubation, the cells were washed in PBS buffer. The platelets were finally resuspended in the same buffer and

analyzed on a FACSCalibur fluorescence cytometer using Cell Quest software (Becton Dickinson, San Jose, CA). Light scatter and fluorescence intensity were recorded for 10 000 platelets on a logarithmic gain.

Cytosolic Calcium Measurements. Cytosolic calcium measurements were performed on immortalized human microvascular endothelial cells (HMECs) cultured in DMEM/F12 medium, 10% human serum, 100 units/mL penicillin, 100 μ g/mL streptomycin, 0.3 mg/mL glutamin, and 1 mM MgSO₄ (Gibco BRL, Cergy-Pontoise, France). Briefly, cultured cells were washed twice in PBS without Ca²⁺ or Mg²⁺ and loaded with 5 μ M Fura-2/acetoxymethyl ester (Calbiochem) in basal salt solution [BSS, 25 mM HEPES (pH 7.3), 125 mM NaCl, 5 mM KCl, 1 mM MgCl₂, 5 mM glucose, and 0.1% fatty acid-free human serum albumin] for 1 h at 37 °C in the dark. HMECs were then detached from culture dishes by incubation with a 5 mM EGTA/1 mM EDTA solution for 15 min at 37 °C. After centrifugation for 5 min at 100g, cells were resuspended at a density of 2×10^6 cells/mL in BSS containing 2 mM CaCl₂ and allowed to equilibrate for 30 min at 37 °C. The intracellular concentration of calcium was measured under constant stirring, using a PTI deltascan spectrofluorimeter (Photon Technology International Inc, Princeton, NJ). Excitation wavelengths were set at 340 and 380 nm, and the emission wavelength was set at 510 nm.

RESULTS

Production of Recombinant PAR1 and PAR2 NH₂-Terminal Exodomains in *E. coli*. Entire NH₂-terminal extracellular domains of mature PAR1 (PAR1E, residues 25–99; 4) and PAR2 (PAR2E, residues 31–79; 24) were produced in *E. coli* as GST fusion proteins (Figure 1A) using the PGEX-6P expression system. The PAR1E and PAR2E polypeptides were released from GST in a single step which involved binding of the fusion protein to glutathione-Sepharose, cleavage of the PAR fragment by prebound PreScission protease, and elution of the cleaved polypeptide. A 150 mL bacterial suspension typically yielded about 1.5 mg of receptor protein. PAR1E and PAR2E were >90% pure as judged by SDS–PAGE, and the apparent molecular masses (\approx 10 and 6 kDa, respectively) agreed with the amino acid compositions (Figure 1B and data not shown). PAR1E was cleaved by thrombin to produce a 7 kDa fragment (Figure 1B), whereas PAR2E was insensitive to thrombin

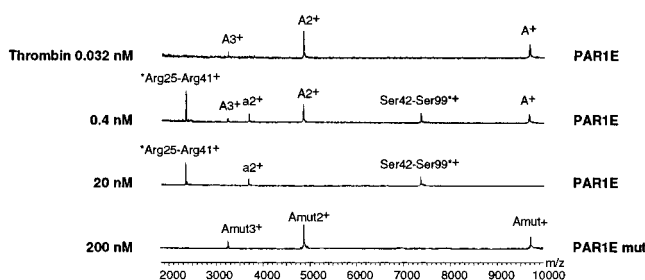


FIGURE 2: Linear MALDI-TOF mass spectra of recombinant PAR1E and PAR1E S42P thrombin cleavage fragments. HPLC-purified PAR1E (10 μ M) or PAR1E mutated at the activation site (PAR1Emut, 10 μ M) was treated for 30 s at 37 $^{\circ}$ C with purified human α -thrombin at the indicated concentrations in 100 mM Tris-HCl (pH 8). A refers to the uncleaved Arg25–Ser99 polypeptide and a to the Ser42–Ser99 fragment. An asterisk indicates amino acids added by the vector construct (see Figure 1).

(data not shown). A Ser to Pro mutation introduced at the P'1 site of PAR1 (PAR1E S42P) or PAR2 (PAR2E S37P) prevented cleavage by their respective native proteases (Figures 1B, 2, and 7).

Characterization of Recombinant PAR1E and PAR2E by LC–MS. To facilitate precise location of the cleavage sites, the polypeptides were further purified to a single molecular species by reverse phase HPLC. On-line LC–MS gave masses of 9731.6 and 6065.8 Da for PAR1E and PAR2E, respectively, which agreed well with the theoretical mass (9731.7 and 6065.9 Da, respectively) calculated from the amino acid sequences (PAR1 residues 25–99 plus 12 amino acids added by the vector construct and PAR2 residues 31–79 plus 11 amino acids added by the vector construct, Figure 1A). The active site Ser \rightarrow Pro mutants had masses of 9741.6 Da (PAR1E S42P) and 6076 Da (PAR2E S37P), consistent with the \approx 10 Da increase caused by the exchange of Ser (105.09 Da) for Pro (115.13 Da). The identities of the four polypeptides were further confirmed by NH₂-terminal amino acid sequencing (PAR1E), or by mass analysis of the partly degraded species isolated during HPLC purification.

Identification of Cleavage Sites by MALDI-MS. HPLC-purified PAR1E and PAR2E (10 μ M) were treated in solution with increasing concentrations of a series of proteases known with the exception of trypsin to be found in the vasculature: thrombin, plasmin, calpain, cathepsin G, elastase, and proteinase 3. This allowed determination of the lowest active concentration of each enzyme, as illustrated for thrombin and PAR1E in Figure 2, which was subsequently used to perform kinetic studies. The shortest incubation time, corresponding to the minimum delay between enzyme addition and removal of an aliquot for TFA quenching, was 30 s, and the incubation period was extended up to 3 h. In most cases, the cleavage sites could be unambiguously derived from the theoretical masses of single cleaved fragments. Occasionally when an experimental mass was found to fit two different putative cleavage peptides, ambiguities were resolved by searching the mass signal of the complementary cleaved fragment(s), or by comparing with an equivalent fragment from Ser \rightarrow Pro mutant PAR. To facilitate comparison and identify the most sensitive sites, the cleavages were divided into early (occurring between 30 s and 5 min) and late (occurring between 5 min and 3 h) (Table 1). The PAR1E S42P and PAR2E S37P mutants containing nonfunctional activation sites were analyzed in parallel with

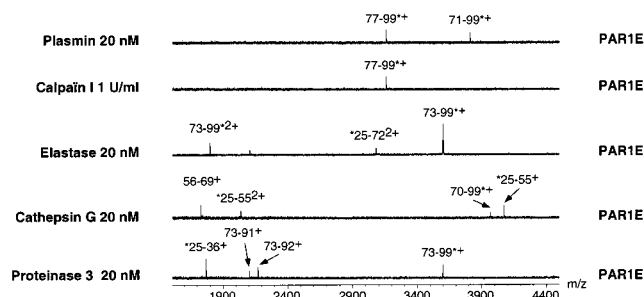


FIGURE 3: Reflector MALDI-TOF mass spectra of the PAR1E fragments generated by plasmin, calpain, elastase, cathepsin G, and proteinase 3. PAR1E (10 μ M) was incubated for 5 min at 37 $^{\circ}$ C with plasmin, calpain, elastase, cathepsin G, or proteinase 3 at the indicated concentrations in 100 mM Tris-HCl (pH 8). An asterisk indicates amino acids added by the vector construct (see Figure 1).

the wild-type peptides and provided an additional means of assessing cleavage outside the activation sites.

Analysis of PAR1E Cleavage by MALDI-MS. Thrombin treatment of PAR1E gave two fragments corresponding to single cleavage between residues 41 and 42 (Figure 2). Some cleavage was already observed after 30 s and for a thrombin concentration as low as 0.16 nM (data not shown), while increasing the concentration to up to 200 nM resulted in complete digestion of PAR1E with an identical peptide fragment pattern. The Ser42 \rightarrow Pro mutation totally abolished cleavage for thrombin concentrations as high as 1 μ M. Trypsin, a known activator of PAR1, and cathepsin G also cleaved after Arg41, but these two enzymes further cleaved at two COOH-terminal positions (Figures 3 and 4 and Table 1). As in thrombin digestion, the Ser42 \rightarrow Pro mutation completely blocked trypsin and cathepsin G cleavage at Arg41. Plasmin, elastase, proteinase 3, and calpain did not affect the activation site but cleaved at sites NH₂- and COOH-terminal to the Arg41–Ser42 site. Thus, our results indicated that all the proteases tested with the exception of thrombin could be expected to inactivate PAR1 at the cell surface, since they all cleaved at a position COOH-terminal to the activation site and at early time points.

Analysis of PAR1E Cleavage and Interaction with Thrombin by Surface Plasmon Resonance. Functionalities of cleavages determined in solution by mass spectrometry were further studied on surface-immobilized PAR1E using the Biacore instrument. A His tag was added at the C-termini of PAR1E and PAR1E S42P, allowing attachment on a Ni²⁺ activated chip as shown in Figure 5. In agreement with the results in solution, thrombin (90 nM), plasmin (500 nM), or elastase (20 nM) efficiently cleaved surface-bound PAR1E as shown by a steep decrease in RU compared with conditions where proteases were incubated with specific inhibitors (Figure 5A). Three minutes after injection, the decrease in RU was on average 35, 50, and 60% for thrombin, plasmin, and elastase, respectively, when compared with the results of buffer injection. Curves obtained with inhibitors were subtracted to evaluate the extent of cleavage. They were superimposable on those obtained with buffer injection (data not shown) and showed a slow desorption (5 RU/min) of immobilized protein on the NTA sensor chip as already documented (31). His-PAR1E S42P could not be cleaved by thrombin but could be cleaved by plasmin and elastase (Figure 5B). To derive kinetic constants for PAR1E

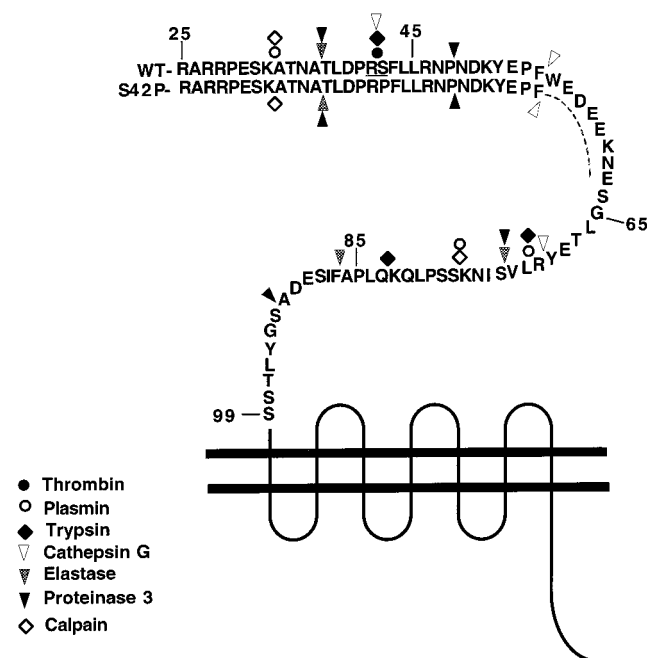


FIGURE 4: Location of the cleavage sites of thrombin, plasmin, calpain, elastase, trypsin, cathepsin G, and proteinase 3 on the NH₂-terminal exodomain of PAR1. Schematic representation and amino acid sequence of the NH₂-terminal fragment of PAR1. WT refers to the native sequence and S42P to PAR1 mutated at the thrombin activation site (underlined), and the numbering corresponds to the mature protein. Amino acids added by the vector have been omitted for simplicity. Protease cleavage sites were identified by MALDI-MS as described in Experimental Procedures, and only the early cleavages of each enzyme are indicated (see Table 1).

binding to thrombin without the added complexity of receptor cleavage, a series of experiments was performed using (i) immobilized His-PAR1E and injection of active site mutant S205A thrombin (32) and (ii) immobilized His-PAR1E S42P and injection of native thrombin or inactive S205A thrombin (Figure 5C). Analysis of the association and dissociation curves provided K_D estimates in the 10^{-7} M range for the three conditions, giving a slightly lower affinity for the combination of mutant thrombin and mutant PAR1E due to the increased dissociation rate (Figure 5D).

Analysis of PAR1 Cleavage at the Platelet Surface. To extend results for the recombinant PAR1E polypeptide to effects on the native receptor, we performed FACS analyses of platelets. Two MoAbs were employed which recognize separate epitopes on the PAR1 exodomain corresponding to residues 32–46 (MoAb IIa-RA) and residues 51–64 (MoAb WEDE; 34). Both antibodies bound to resting human platelets and gave a fluorescence signal in agreement with the estimated PAR1 surface density of ≈ 1800 copies/platelet (35). Thrombin treatment induced a loss of IIa-RA binding (Figure 6A) but had no effect on WEDE binding (data not shown), consistent with cleavage between positions 41 and 42. All the other enzymes destroyed the epitopes of both IIa-RA (data not shown) and WEDE (Figure 6B–F). This indicated cleavage downstream of positions 51–64, in complete agreement with the MALDI-MS analysis which had identified at least one cleavage site beyond residue 65 for all these enzymes.

Analysis of PAR2E Cleavage by MALDI-MS. HPLC-purified PAR2E and PAR2E S37P were cleaved and

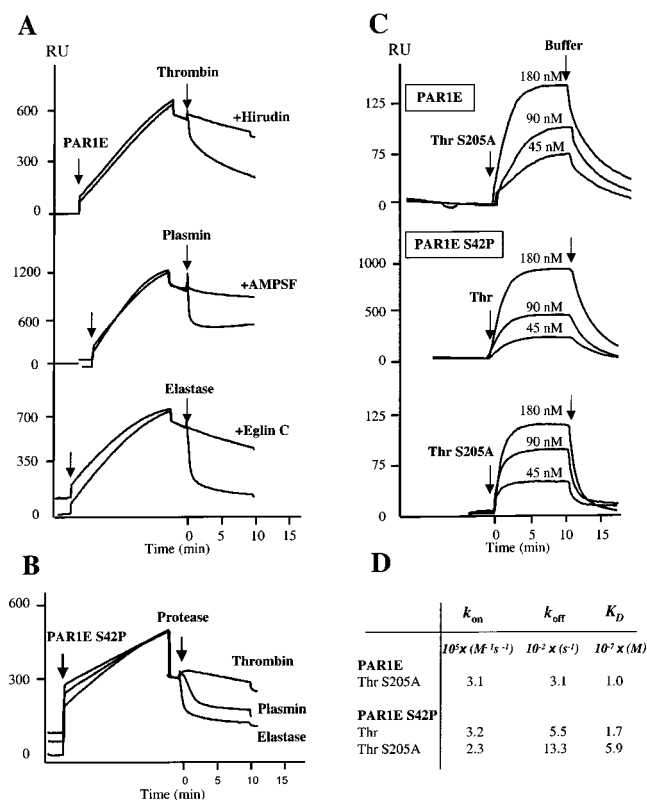


FIGURE 5: Surface plasmon resonance analysis of PAR1E cleavage by thrombin, plasmin, and elastase and kinetic properties of PAR1E–thrombin binding. Sensorgrams were recorded on a Biacore 2000 apparatus using a Ni²⁺-activated NTA sensor chip by perfusing 200 nM His-tagged PAR1E or PAR1E S42P for 15 min followed by addition of proteases. (A) Cleavage of immobilized PAR1E was tested by injecting (upper curve) thrombin (90 nM) with or without 20 units/mL hirudin, (middle curve) plasmin (500 nM) with or without APMSF (20 μ M), or (lower curve) elastase (20 nM) with or without eglin C (10 μ g/mL). (B) Cleavage of His-PAR1E S42P was tested as described for panel A in the absence of inhibitors. (C) Kinetic studies of the interaction of immobilized PAR1E (upper curve) or PAR1E S42P (middle and lower curves) with native thrombin (Thr, middle curve) or active site mutant S205A thrombin (Thr S205A, upper and lower curves). Thrombin was injected following binding of His-PAR1E or His-PAR1E S42P, and resonance units levels were adjusted to baseline. (D) Association (k_{on}) and dissociation (k_{off}) constants and K_D values for PAR1E–Thr S205, PAR1E S42P–Thr, and PAR1E S42P–Thr S205A interactions were derived from analysis of panel C using Biaevaluation software.

analyzed by mass spectrometry as described for PAR1E. Trypsin cleaved PAR2E at the Arg36–Ser37 activation site and at two additional downstream cleavage sites corresponding to the Lys51–Gly52 and Lys72–Leu73 sites (Figure 7). Cleavage was also observed at the Arg36–Ser37 site for high thrombin concentrations (200 nM) or long incubation times (3 h) (Table 1). Two plasmin cleavage sites were located one amino acid upstream and at the activation site (positions 34 and 35, and 36 and 37, respectively). All the other enzymes cleaved at a position COOH-terminal to the activation site, at one position for elastase, two for cathepsin G, and four for proteinase 3 (Table 1). Calpain only cleaved at high concentrations and for long incubation times. According to these results, it can be predicted that plasmin and trypsin might display both activating and inhibitory properties, while the three leukocyte proteases should inactivate the receptor.

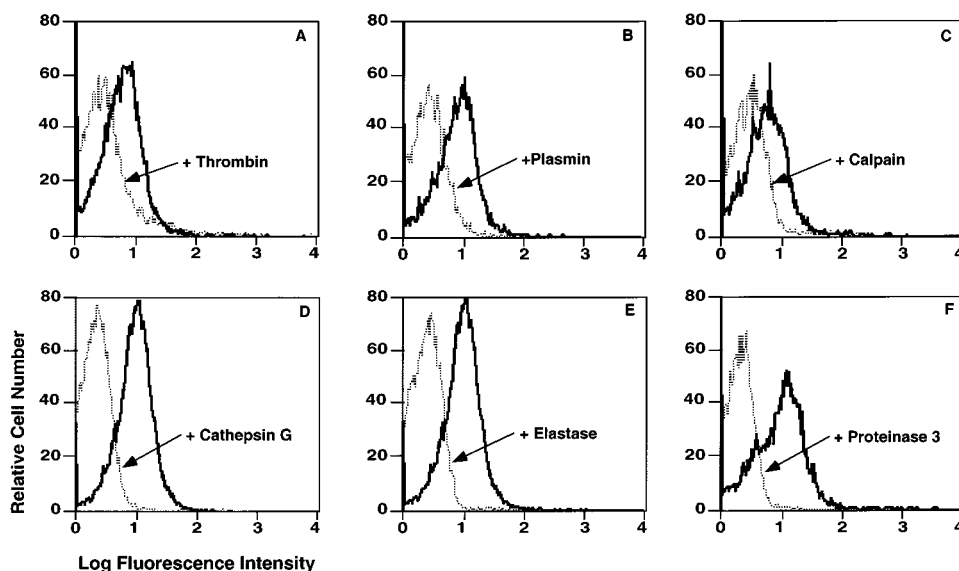


FIGURE 6: Protease cleavage of the NH₂-terminal exodomain of PAR1 at the surface of platelets. Resting platelets (thick lines) or platelets treated with thrombin (5 min) or other proteases (30 min) at 37 °C (dashed lines) were incubated with the MoAb IIa-RA recognizing the Arg41–Ser42 PAR1 activation site (A) or WEDE directed against an epitope COOH-terminal to the activation site (B–F). Thrombin cleaved at the Arg41–Ser42 site and destroyed the IIa-RA epitope (A). All the other proteases cleaved downstream from the activation site and removed the WEDE epitope from the platelet surface (B–F).

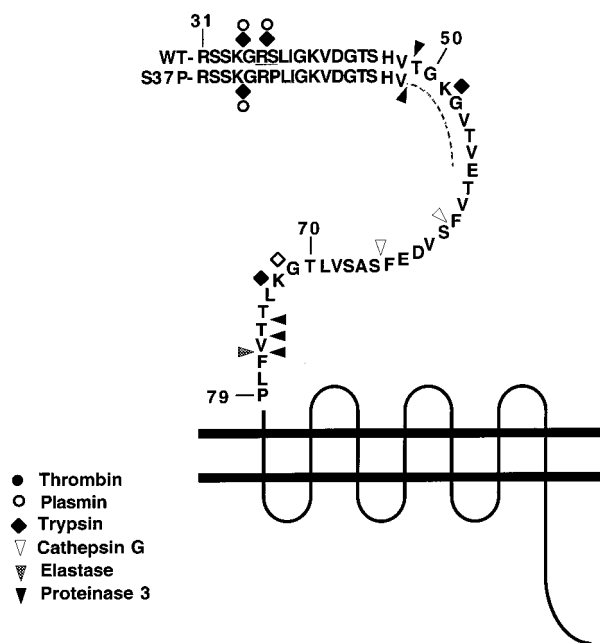


FIGURE 7: Location of the cleavage sites of thrombin, plasmin, elastase, trypsin, cathepsin G, and proteinase 3 on the NH₂-terminal exodomain of PAR2. Schematic representation and amino acid sequence of the NH₂-terminal fragment of PAR2. WT refers to the native sequence and S37P to PAR2 mutated at the trypsin activation site (underlined), and the numbering corresponds to the mature protein. Amino acids added by the vector have been omitted for simplicity. Protease cleavage sites were identified by MALDI-MS as described in Experimental Procedures and only the early cleavages of each enzyme are indicated (see Table 1).

Effect of Elastase on PAR1 and PAR2-Dependent Calcium Signaling. Mass spectrometry analysis predicted inactivation of both PAR1 and PAR2 by the series of leukocyte proteases. To test this hypothesis, Ca²⁺ signaling studies were performed on the HMEC endothelial cell line which was found to express functional PAR1 and PAR2. Addition of thrombin (0.1 unit/mL) followed 10 min later by trypsin (50 nM) produced two Ca²⁺ peaks with similar amplitudes (Figure

8A). A second thrombin stimulation was not followed by a Ca²⁺ peak due to PAR1 desensitization (data not shown). This showed that the trypsin response was independent of PAR1 when performed 10 min after thrombin stimulation and was likely caused by PAR2. Elastase treatment for 10 min had no effect on Ca²⁺ levels at concentrations as high as 250 nM but dose-dependently abrogated the response to thrombin. The trypsin response was also decreased down to 45% of control after treatment with 250 nM elastase. A residual response to trypsin was similarly observed when PAR1 and PAR2 were inactivated by successive treatment with thrombin and the SLIGR peptide.

DISCUSSION

Extracellular proteinases play a crucial role in the regulation of numerous physiological processes such as embryogenesis, tissue remodeling, and hemostasis (1). In this study, we tested proteases likely to be encountered in the vasculature for their ability to activate or inhibit members of the newly described PAR family of receptors. PARs differ from other G protein-coupled receptors in being essentially single-use receptors since their activation requires an intact NH₂-terminus. Once cleaved, these receptors cannot regain functional potential, although intracellular pools can be mobilized as has been shown for PAR1 in vascular endothelial cells (36) and megakaryocytic cell lines (34). In the case of platelets, however, the intracellular pool of receptors is very limited, and these cells are almost incapable of protein synthesis (37). A protease which cleaves at the wrong site will inactivate or disarm the receptor and prevent its subsequent cleavage by the activating protease. Hence, the ability of certain proteases to downregulate the activity of PARs could be one of the mechanisms developed by nature to modulate hemostatic and vascular responses. Studies of the modes of activation and inactivation of PARs are therefore important in better understanding the physiology of this new class of receptors and for their pharmacological manipulation.

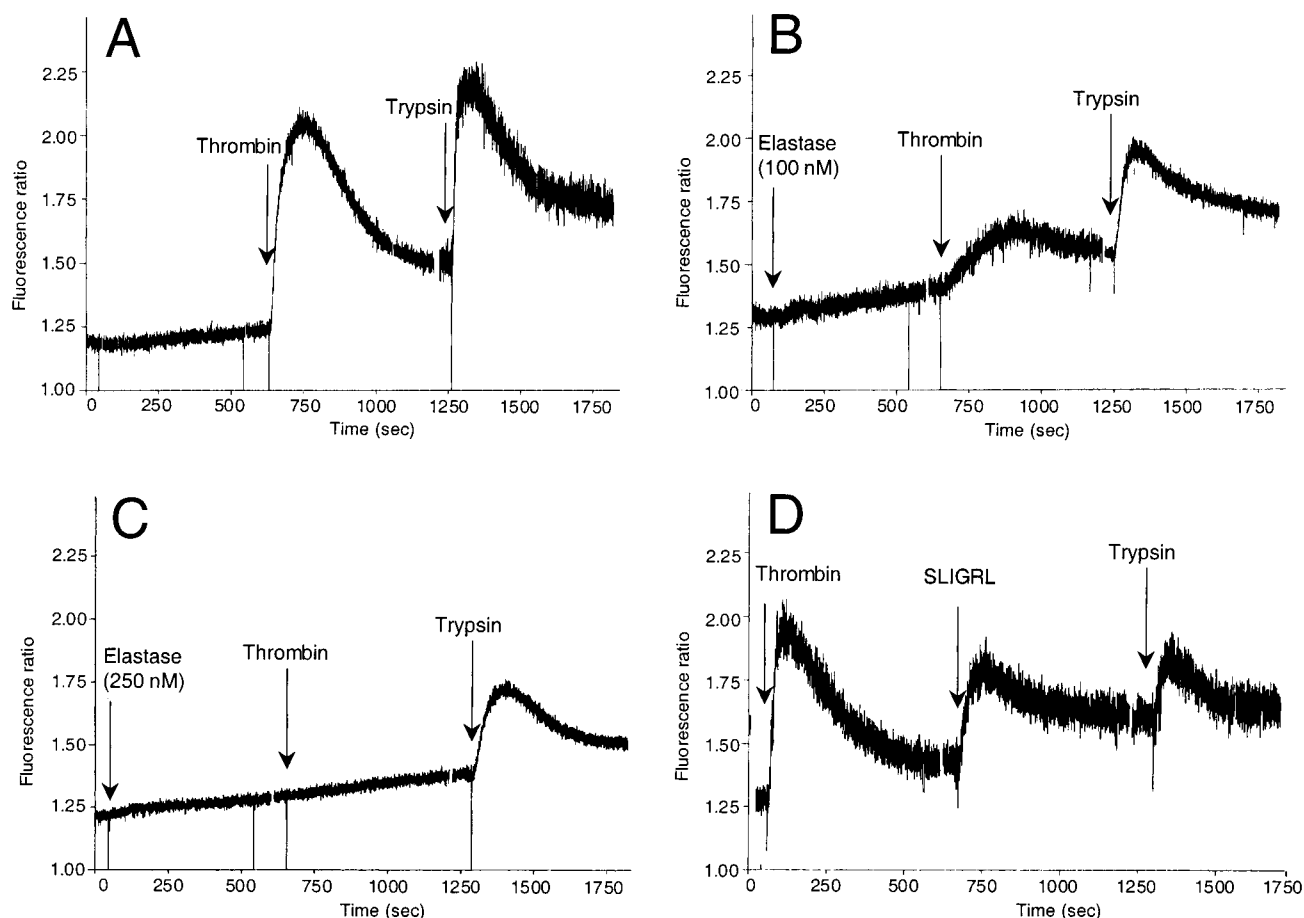


FIGURE 8: PAR1 and PAR2 Ca^{2+} responses in the HMEC endothelial cell line after treatment with elastase. HMECs loaded with the Fura-2 Ca^{2+} indicator were incubated with the indicated proteases at 10 min intervals. (A) Cells were sequentially treated with buffer, 0.1 unit/mL thrombin, and 50 nM trypsin producing two Ca^{2+} peaks characteristic of PAR1 and PAR2 responses, respectively. Pretreatment with 100 nM (B) and 250 nM (C) elastase progressively abolished the response to thrombin and decreased the response to trypsin. Activity of elastase was blocked by eglin C after incubation for the first 10 min. (D) Successive treatment with thrombin and the PAR2 activating SLIGRL peptide only partially blocked the response to trypsin.

Previous investigations of PAR1 and PAR2 cleavage employed short synthetic peptides corresponding to the first exodomain (4, 18–20). Use of such synthetic peptides is nevertheless associated with a risk of detecting artificial cleavage due to the lack of a native conformation or of missing true cleavage sites due to the incorrect design of the peptide boundaries. Since earlier studies of PAR1 had demonstrated that the NH_2 -terminal exodomain contained all the information needed for efficient recognition and cleavage by thrombin, its physiologic agonist (21, 22), we used recombinant techniques to express in *E. coli* the entire NH_2 -terminal exodomains of PAR1 (PAR1E) and PAR2 (PAR2E), which could be expected to adopt a more native conformation than short peptides. In fact, a His-tagged PAR1 Arg26–Gln81 fragment has been proposed as a surrogate for the intact receptor in biochemical and kinetic studies of receptor cleavage (21). PAR1E and PAR2E were produced by an improved procedure allowing almost pure proteins to be obtained in a single chromatographic step. An additional HPLC purification step gave a single molecular species, a necessary requirement for the accurate identification of protease cleavage sites by mass spectrometry. As compared to studies using synthetic peptides, 10–20-fold lower concentrations of enzymes were needed to cleave the recombinant proteins (refs 18–20 and 37 and data not

shown), which would suggest a more native conformation adopted by the complete exodomains.

Native NH_2 -terminal exodomains of PAR1 and PAR2 contain N-linked glycosylation sites which could theoretically modify cleavage sites. Nonetheless, the results strongly suggest that the recombinant PAR extracellular domains can substitute for the intact receptor in the study of interaction and cleavage by proteases. This was supported by the observation that concentrations of proteases that are active on the native platelet receptor efficiently cleaved the recombinant PAR1E. These data obtained in solution were confirmed on surface-immobilized PAR1E by surface plasmon resonance (SPR) analysis. This technique allowed kinetic studies of PAR1E cleavage which agreed with mass spectrometry results and also allowed estimation of thrombin–PAR1E affinities by the use of active site mutant thrombin and inactivated PAR1E S42P. The 10^{-7} M values obtained are in keeping with K_m values obtained with cleavable recombinant polypeptides (21, 45) and close to concentrations of thrombin known to activate cells.

Use of MALDI-MS technology was essential to the study presented here. This technique offers several advantages over traditional approaches, necessitating the purification of cleaved peptides and NH_2 -terminal amino acid identification. The MALDI-MS procedure eliminates the need to purify the

cleaved reaction mixture and allows direct identification of the peptides on a single sample due to the extreme accuracy of the mass determination. This experimentally simple approach can, if needed, produce measurements every 30 s which can be useful in determining early and rapid cleavages usually encountered under physiological situations. In addition, the high sensitivity of the method (low picomolar range) permits use of very small amounts of precious reagents (38), avoiding the constraints of limiting amounts of substrate or enzyme. Finally, a large number of samples can be analyzed in a short period of time. MALDI mass spectra analysis was not intended for precise quantification of the cleavage products but rather for discrimination of the early attack sites. Indeed, it is well established that the response factor varies between different peptides and that the peak intensity does not always correlate with the peptide concentration, making precise quantification hazardous (39).

Proteinases were selected for study on the basis of their presence in the circulation in thrombotic and inflammatory situations and their potential effects on platelets and vascular cells. Thrombin, plasmin, leukocyte elastase, cathepsin G, and proteinase 3 are serine proteases which can come into contact with platelets and endothelial cells (15, 18, 19). The role of serine proteinases in regulating hemostasis has long been recognized in connection with the strong hemostatic action of aprotinin, a member of the serpin family, in cardiac surgical procedures (40), but their cellular effects especially on PARs are still obscure. The MALDI-MS study of PAR1E confirmed the modes of action of some proteinases and provided valuable new information about others. Thus, the known action of thrombin on PAR1 involving cleavage at the Arg41–Ser42 bond was confirmed, and no other cleavage site was found within the NH₂-terminal exodomain of the receptor.

Plasmin mediates the lysis of fibrin clots and could in different studies activate platelets or inhibit the responses induced by thrombin (41–43). Our study favors a net inactivating effect on PAR1 despite minor cleavage at Arg41, on the basis of preferential cleavage at positions Arg70 and Lys76, COOH-terminal to the Arg41–Ser42 activation site. As a consequence, platelets recirculating after release from the fibrin clot through the action of plasmin would not be able to respond to a second thrombin challenge. Two early reports of the cleavage of synthetic peptides of PAR1 residues 40–55 and 38–60 at Arg41 (20, 44) suggested possible activation by plasmin. In a more recent study in which the effects of plasmin on PAR1 residues 25–103 were analyzed (45), this enzyme was found to cleave with equal efficiency at Arg41 and at three COOH distal sites (Arg70, Lys76, and Lys85) and was proposed to have a dual activating and desensitizing role. Differences with the previous study might be explained by the denaturation–refolding procedure used in preparing the recombinant protein (45). The results presented here favor a net inactivating effect of plasmin, which was confirmed in aggregation experiments where treatment with a wide range of plasmin concentrations (up to 500 nM) failed to activate platelets and decreased thrombin-induced responses (data not shown).

Cathepsin G, elastase, and proteinase 3 constitute a group of serine proteases found within the azurophilic granules of neutrophils. Secretion of these proteases can cause degradation of a variety of extracellular matrix macromolecules and

lead to emphysema, rheumatoid arthritis, or atherosclerosis (15, 19). These enzymes may also regulate hemostasis by cleaving clotting factors (46) and modulating platelet activation (15, 18, 19, 47).

Cathepsin G is a well-known platelet agonist, and the hypothesis of the possible existence of a specific cell surface receptor, perhaps belonging to the PAR family, has been raised (18, 19, 48, 49). Peptide studies suggested that cathepsin G could activate or inactivate PAR1 by cleaving at the Arg41–Ser42 (18, 19), Phe43–Leu44 (18), Phe55–Trp56 (18, 19), and Tyr69–Lys70 sites (19). Cleavage at these positions was confirmed using recombinant PAR1E, but kinetic analyses indicated preferential cleavage at the Phe55–Trp56 site. This would support a net inactivating effect of cathepsin G on PAR1 and does not explain its agonistic action on platelets, which could be mediated by another PAR. Very recently, it has been found that PAR4 could act as a cathepsin G receptor (50).

Endothelial PAR2 might also be exposed to cathepsin G during inflammation, and our results suggest like for PAR1 an inhibitory effect through cleavage at Phe59–Ser60 and Phe64–Ser65 sites COOH-terminal to the activation site. The concentrations of cathepsin G estimated to be present at sites of vascular injury (0.5 μ M) may be expected from this study to desensitize PAR1 and PAR2, neither of which displays the properties of a potential cathepsin G receptor.

Elastase does not directly activate platelets but potentiates their activation by cathepsin G (49). This effect is probably not mediated through PAR1, since elastase digestion of PAR1E resulted in multiple cleavages at Ala36–Thr37, Val72–Ser73, and Ala86–Phe87 sites with preferential cleavage at Val72, which would disable the receptor. The same sites were described in a previous study (19) with the exception of the Ala36 cleavage which was missed due to peptide design. Cleavage at positions COOH-terminal to the activating site was confirmed on the native receptor by the disappearance of the Arg41–Ser42 epitope on platelets treated with elastase and by a decreased Ca²⁺ response to thrombin in elastase-treated HMECs.

The role of proteinase 3 (51) in vascular cell function has received less attention. In our study, the multiple COOH-terminal cleavages of the first exodomains again implied inactivation of PAR1 and PAR2. As compared to results for synthetic peptides, four additional cleavages were found on PAR1E with a majority located COOH-terminal to Arg41 (19), while no alternative data were available for PAR2. Thus, our results indicate that the main serine proteases secreted from activated neutrophils and present in inflammatory situations should have an overall inhibitory effect on the cell activation mediated by PAR1 and PAR2.

Calpain is a ubiquitous Ca²⁺-activated proteinase now increasingly implicated as a modulator of cell adhesion and motility. Cleavages of adhesive receptors such as integrins or of actin-associated proteins are examples of the Ca²⁺-regulated functions of calpain (52–55). To our knowledge, the role of calpain in modulating responses to G protein-coupled receptors is unknown. This study shows that calpain can participate in terminating or blocking thrombin signaling by cleaving PAR1 at Lys76, and this site would appear from platelet FACS analyses to be functional.

Less information is available concerning the sensitivity of PAR2 to proteases than in the case of PAR1. Although

the tissue distribution suggests that trypsin is unlikely to be the sole protease capable of activating PAR2, the physiologic protease is still unknown (56). Our approach has the potential to identify quickly and with a good level of confidence the natural protease(s) of PAR2. The physiologic relevance of the results obtained using recombinant PAR1E is supported by their good correlation with the cleavage specificities and active concentration ranges of enzymes observed for PAR1 on intact platelets. Therefore, we postulate that the results for PAR2E should mimic the behavior of native PAR2 at the cell surface. Trypsin and plasmin were the only proteases tested which cleaved at the Arg36–Ser37 activation site, indicating the possibility of cell activation by plasmin. Recent results on rat brain capillary endothelial cells demonstrated a lack of Ca^{2+} responses to plasmin despite normal responses to thrombin and the presence of PAR1, PAR2, and PAR3 detected at the mRNA level (57). This study suggested a lack of plasmin response through PAR2 but did not test the possibility of PAR2 inactivation. The lack of response to plasmin could be due to the presence of a second cleavage site at positions 34 and 35 which would predict an inefficient response to trypsin. This study (57) also demonstrated that plasmin pretreatment decreased the Ca^{2+} response to thrombin which was predicted from the present study on the basis of cleavage COOH-terminal to Ser42.

As stated earlier, enzymes encountered in inflammatory situations such as elastase, cathepsin G, and proteinase 3 should further blunt the responses mediated by PAR2. Indeed, treatment of the HMEC cell line with elastase decreased the Ca^{2+} responses to trypsin under conditions where the PAR1 response was blunted, an effect probably due to PAR2 inactivation. The trypsin response could not be completely abolished by elastase treatment, suggesting the presence of an alternate receptor. This hypothesis was reinforced by the observation of a residual trypsin response following desensitization of PAR2 by the SLIGRL peptide.

The effects of proteases on the newly cloned PAR3 (9) and PAR4 (7, 8) thrombin receptors are still unknown and would be readily evaluated using the strategy presented here. The same approach could be equally useful in studying other protease-related systems or substrates.

This work also provides information about the peptide bond recognition of different proteases. As expected, thrombin cleaved preferentially after Arg and plasmin after Arg and Lys residues. Cathepsin G, elastase, and proteinase 3 belong to the same family and prefer hydrophobic residues at the P1 site but had different primary amino acid specificities (58, 59). Cathepsin G cleaved preferentially after aromatic residues (Phe and Trp), while elastase cleaved at bonds where the P1 residue had a small alkyl side chain (Ala and Val), as did proteinase 3 which also cleaved efficiently after Thr and Pro. No real consensus cleavage site has been described for calpain, and this was confirmed here by the indifferent cleavage after basic (Lys in PAR1E) or uncharged (Val and Gly in PAR2E) residues. Apparently, the strict specificity of this enzyme for its different substrates depends more on a high degree of structural order, and small molecules are poor substrates for calpain (17).

ACKNOWLEDGMENT

We thank Juliette Mulvihill for correcting the English.

REFERENCES

1. Werb, Z. (1997) *Cell* 91, 439–442.
2. Coughlin, S. R. (1999) *Thromb. Haemostasis* 82, 353–356.
3. Chesebro, J. H., Zoldhelyi, P., Badimon, L., and Fuster, V. (1991) *Thromb. Haemostasis* 66, 1–5.
4. Vu, T. H., Hung, D. T., Wheaton, V. I., and Coughlin, S. R. (1991) *Cell* 64, 1057–1068.
5. Ishihara, H., Connolly, A. J., Zeng, D., Kahn, M. L., Zheng, Y. W., Timmons, C., Tram, T., and Coughlin, S. R. (1997) *Nature* 386, 502–506.
6. Shmidt, V. A., Niernan, W. C., Maglott, D. R., Cupit, L. D., Moskowitz, K. A., Wainer, J. A., and Bahou, W. F. (1998) *J. Biol. Chem.* 273, 15061–15068.
7. Kahn, M. L., Zheng, Y. W., Huang, W., Bigornia, V., Zeng, D., Moff, S., Farese, R. V., Tam, C., and Coughlin, S. R. (1998) *Nature* 394, 690–694.
8. Xu, W.-F., Andersen, H., Whitmore, T. E., Presnell, S. R., Yee, D. P., Ching, A., Gilbert, T., Davie, E., and Foster, D. C. (1998) *Proc. Natl. Acad. Sci. U.S.A.* 95, 6642–6646.
9. Kahn, M. L., Hammes, S. R., Botka, C., and Coughlin, S. R. (1998) *J. Biol. Chem.* 273, 23290–23296.
10. Nystedt, S., Emilsson, K., Wahlestedt, C., and Sundelin, J. (1994) *Proc. Natl. Acad. Sci. U.S.A.* 91, 9208–9212.
11. Mirza, H., Yatsula, V., and Bahou, W. J. (1996) *J. Clin. Invest.* 97, 1705–1714.
12. Molino, M., Woolkalis, M. J., Reavey-Cantwell, J., Pratico, D., Andrade-Gordon, P., Barnathan, E. S., and Brass, L. F. (1997) *J. Biol. Chem.* 272, 11133–11141.
13. Gaffney, P. J., and Longstaff, C. (1994) in *Haemostasis and Thrombosis* (Bloom, A. L., Forbes, C. D., Thomas, D. P., and Tuddenham, E. G. D., Eds.) 3rd ed., pp 549–573, Churchill Livingstone, Edinburgh, U.K.
14. Borregaard, N., Lollike, K., Kjeldsen, L., Sengelov, H., Bastholm, L., Nielsen, M. H., and Bainton, D. F. (1993) *Eur. J. Haematol.* 51, 187–198.
15. Cerletti, C., Evangelista, V., Molino, M., and de Gaetano, G. (1995) *Thromb. Haemostasis* 74, 218–223.
16. Fox, J. E. B., Goll, D. E., Reynolds, C. C., and Phillips, D. R. (1985) *J. Biol. Chem.* 260, 1060–1066.
17. Saido, T. C., Sorimachi, H., and Suzuki, K. (1994) *FASEB J.* 8, 814–822.
18. Molino, M., Blanchard, N., Belmonte, E., Tarver, A. P., Abrams, C., Hoxie, J. A., Cerletti, C., and Brass, L. F. (1995) *J. Biol. Chem.* 270, 11168–11175.
19. Renesto, P., Si-Tahar, M., Moniatte, M., van Dorsselaer, A., Pidard, D., and Chignard, M. (1997) *Blood* 89, 1944–1953.
20. Parry, M. A. A., Myles, T., Tschopp, J., and Stone, S. R. (1996) *Biochem. J.* 320, 335–341.
21. Ishii, K., Gerszten, R., Zheng, Y. W., Welsh, J. B., Turck, C. W., and Coughlin, S. R. (1995) *J. Biol. Chem.* 270, 16435–16440.
22. Bahou, W. F., Collier, B. S., Potter, C. L., Norton, K. J., Kutok, J. L., and Goligorsky, M. S. (1993) *J. Clin. Invest.* 91, 1405–1413.
23. Bouton, M.-C., Jandrot-Perrus, M., Moog, S., Cazenave, J.-P., Guillin, M.-C., and Lanza, F. (1995) *Biochem. J.* 305, 635–641.
24. Nydstedt, S., Emilsson, K., Larsson, A. K., Strombeck, B., and Sundelin, J. (1995) *Eur. J. Biochem.* 232, 84–89.
25. Nachon, F., Ehret-Sabatier, L., Loew, D., Colas, C., van Dorsselaer, A., and Goeldner, M. (1998) *Biochemistry* 37, 10507–10513.
26. Kussmann, M., Lassing, U., Sturmer, C. A., Przybylski, M., and Roepstorff, P. (1997) *J. Mass Spectrom.* 32, 483–493.
27. Vorm, O., Roepstorff, P., and Mann, M. (1994) *Anal. Chem.* 66, 3281–3287.
28. Vorm, O., and Mann, M. (1994) *J. Am. Soc. Mass Spectrom.* 5, 955–958.
29. Karas, M., and Hillenkamp, F. (1988) *Anal. Chem.* 60, 2299–2301.
30. Ravanat, C., Morales, M., Azorsa, D. O., Moog, S., Schuhler, S., Grunert, P., Loew, D., van Dorsselaer, A., Cazenave, J.-P., and Lanza, F. (1997) *Blood* 89, 3253–3262.

31. Nieba, L., Nieba-Axmann, S. E., Persson, A., Hämäläinen, M., Edebratt, F., Hansson, A., Lidholm, J., Magnusson, K., Karlsson, A. F., and Plückthun, A. (1997) *Anal. Biochem.* 252, 217–228.
32. Arone, R., Pagliuca, M. G., Chinali, A., Grimaldi, M., Schettini, G., Gast, A., and Pietropaolo, C. (1999) *Biochim. Biophys. Acta* 1451, 173–186.
33. Lanza, F., Beretz, A., Stierlé, A., Hanau, D., Kubina, M., and Cazenave, J.-P. (1988) *Am. J. Physiol.* 225, H1276–H1288.
34. Hoxie, J. A., Ahuja, M., Belmonte, E., Pizzaro, S., Paryon, R., and Brass, L. F. (1993) *J. Biol. Chem.* 268, 13756–13763.
35. Brass, L. F., Vassallo, R. R., Jr., Belmonte, E., Ahuja, M., Cichowski, K., and Hoxie, J. A. (1992) *J. Biol. Chem.* 267, 13795–13798.
36. Woolkalis, M. J., DeMelfi, T. M., Blanchard, N., Hoxie, J. A., and Brass, L. F. (1995) *J. Biol. Chem.* 270, 9868–9875.
37. Molino, M., Bainton, D. F., Hoxie, J. A., Coughlin, S. R., and Brass, L. F. (1997) *J. Biol. Chem.* 272, 6011–6017.
38. Stults, J. T. (1995) *Curr. Opin. Struct. Biol.* 5, 691–698.
39. Krause, E., Wenschuh, H., and Jungblut, P. R. (1999) *Anal. Chem.* 71, 4160–4165.
40. Royston, D. (1990) *Blood Coagulation Fibrinolysis* 1, 55–69.
41. Penny, W. F., and Ware, J. A. (1992) *Blood* 79, 91–98.
42. Kinlough-Rathbone, R. L., Perry, D. W., Rand, M. L., and Packham, M. A. (1997) *Thromb. Haemostasis* 77, 741–747.
43. Nakamura, K., Kimura, M., Fenton, J. W., Andersen, T. T., and Aviv, A. (1995) *Am. J. Physiol.* 268, C958–C967.
44. Kimura, M., Andersen, T. T., Fenton, J. W., Bahou, W. F., and Aviv, A. (1996) *Am. J. Physiol.* 271, C40–C60.
45. Kuliopoulos, A., Covic, L., Seeley, S. K., Sheridan, P. J., Helin, J., and Costello, C. E. (1999) *Biochemistry* 38, 4572–4585.
46. Camire, R. M., Kalafatis, M., and Tracy, P. B. (1998) *Biochemistry* 37, 11896–11906.
47. Weksler, B. B., Jaffe, E. A., Brower, M. S., and Cole, O. G. (1989) *Blood* 74, 1627–1634.
48. Selak, M. A. (1994) *Biochem. J.* 297, 269–275.
49. Renesto, P., and Chignard, M. (1993) *Blood* 82, 139–144.
50. Sambrano, G. R., Huang, W., Faruqi, T., Mahrus, S., Craik, C., and Coughlin, S. (2000) *J. Biol. Chem.* 275, 6819–6823.
51. Renesto, P., Halbwachs-Mecarelli, L., Nusbaum, P., Lesavre, P., and Chignard, M. (1994) *J. Immunol.* 152, 4612–4617.
52. Schoenwalder, S. M., Yuan, Y., Cooray, P., Salem, H. H., and Jackson, S. P. (1997) *J. Biol. Chem.* 272, 1694–1702.
53. Huttenlocher, A., Palecek, S. P., Lu, Q., Zhang, W., Mellgren, R. L., Lauffenburger, D. A., Ginsberg, M. H., and Horwitz, A. F. (1997) *J. Biol. Chem.* 272, 32719–32722.
54. Stewart, M. P., McDowall, A., and Hogg, N. (1998) *J. Cell Biol.* 140, 699–707.
55. Potter, D. A., Tirnauer, J. S., Janssen, R., Croall, D. E., Hughes, C. N., Fiaccio, K. A., Mier, J. W., Maki, M., and Herman, I. M. (1998) *J. Cell Biol.* 141, 647–662.
56. Cupit, L. D., Schmidt, V. A., and Bahou, W. F. (1999) *Trends Cardiovasc. Med.* 9, 42–48.
57. Bartha, K., Dömötör, E., Lanza, F., Adam-Vizi, V., and Machovich, R. (2000) *J. Cereb. Blood Flow Metab.* 20, 175–182.
58. Nakajima, K., Powers, J. C., Ashe, B. A., and Zimmerman, M. (1979) *J. Biol. Chem.* 254, 4027–4032.
59. Kam, C. M., Kerrigan, J. E., Dolman, K. M., Goldschmeding, R., Von dem Borne, A. E. K., and Powers, J. C. (1992) *FEBS Lett.* 297, 119–123.

BI0003341